American Mineralogist, Volume 81, pages 833–841, 1996

Effects of temperature and pressure on the structure of lawsonite

PAOLA COMODI AND PIER FRANCESCO ZANAZZI

Dipartimento di Scienze della Terra, Università di Perugia, Piazza Università, I-06100 Perugia, Italy

ABSTRACT

Independent isobaric data on thermal expansion and isothermal compressibility data for lawsonite, $CaAl_2Si_2O_7(OH)_2 \cdot H_2O$, were determined between 23 and 598 °C and 0.001 and 37.7 kbar using single-crystal X-ray diffraction in a microfurnace and a diamond-anvil cell, respectively. The crystal structures of lawsonite were also refined from intensity data collected at 23, 444, and 538 °C and 0.5 and 28.7 kbar.

Both expansion and compression patterns are slightly anisotropic, with minor changes along c with respect to a and b. Unit-cell dimensions vary linearly with T and P: $\alpha_a = 1.26(4) \times 10^{-5}$, $\alpha_b = 1.12(4) \times 10^{-5}$, $\alpha_c = 7.6(3) \times 10^{-6}$ °C^{-1}, and $\beta_a = 3.4(1) \times 10^{-4}$, $\beta_b = 3.0(1) \times 10^{-4}$, $\beta_c = 2.8(2) \times 10^{-4}$ kbar^{-1}. Bulk modulus, calculated as the reciprocal of cell-volume compressibility, is 1100(40) kbar.

The cavities of the framework accommodating Ca and H_2O molecules change by only about ±5% in the investigated T and P ranges. Thus, at room pressure H_2O molecules can be hosted in the lawsonite structure at least up to above 500 °C, where the reduction of reflection intensities shows the beginning of dehydration and breakdown of the phase.

Like other dense phases, structural changes with T and P essentially affect bond lengths, whereas interpolyhedral variations mainly concern the Si-O-Si′ angle between tetrahedral pairs, which increases with temperature and decreases with pressure.

The present data define the "geometric" equation of state for lawsonite on the basis of cell-volume variations: $V/V_0 = 1 + 3.13(9) \times 10^{-5}T - 9.1(3) \times 10^{-4}P$, where T is in degrees Celsius, P is in kilobars, and the α/β ratio is 34 bar/°C. This indicates that the cell volume of lawsonite remains unchanged with geothermal gradients of about 10 °C/km, a condition actually observed in down-going subduction slabs. Therefore, the results of high-T and high-P structure refinements are in agreement with results from multi-anvil experiments and confirm that lawsonite is a good candidate for carrying water down to mantle depths.

INTRODUCTION

Lawsonite is a common mineral in metabasalts and Ca-rich metagreywackes and is considered as an index mineral of high-pressure, low-temperature metamorphism. In blueschist facies, lawsonite crystallizes in conditions ranging from 0.3 to 1.0 GPa and 150 to 400 °C (Diessel et al. 1978). Recently, results from multi-anvil experiments on the CASH system (Schmidt and Poli 1994; Pawley 1994) have shown that lawsonite is stable to 1040–1080 °C and 92–94 kbar in the P-T regimes observed in most subduction slabs, with the most extreme conditions of 120 kbar and 960 °C (Schmidt 1995). Thus, lawsonite may remain stable during the subduction process in down-going oceanic crust to P exceeding 120 kbar, and its breakdown may contribute to the recycling of water in the mantle above the subduction slabs to depths of more than 200 km (Poli and Schmidt 1995).

The crystal structure of lawsonite, $CaAl_2Si_2O_7(OH)_2 \cdot H_2O$, was determined by Wickman (1947) and later refined by Baur (1978) in space group *Ccmm*. It is based on edge-sharing Al octahedra, forming chains along the [010] direction. These chains are linked by Si_2O_7 groups, and the cavities of the open framework accommodate one Ca atom and one H_2O molecule per formula unit. There are also two OH groups linked to Al octahedra. The total H_2O content is ~11 wt%.

Notwithstanding its close chemical similarity with anorthite, lawsonite has greater density (3.09 instead of 2.76 g/cm^3) and a different Al coordination: octahedral in lawsonite and tetrahedral in anorthite.

The high H_2O content of lawsonite, together with the stability conditions, indicate that this mineral is a good candidate for water storage in subduction slabs in addition to other OH-containing phases like antigorite, magnesiochloritoid, talc, phengite, staurolite, and epidote. Using single-crystal X-ray diffraction techniques to determine the compressibility and thermal expansion of lawsonite, the present study aims to contribute knowledge of lawsonite's structural stability field in P-T space. High-temperature and high-pressure structural refinements also allowed analysis of structural deformations produced by P and T and evaluation of the actual-structural capacity of this phase as a high-P H_2O reservoir.

0003–004X/96/0708–0833$05.00

TABLE 1. Refinement details of lawsonite

P (kbar)	0.001	0.5	28.7	0.001	0.001
T (°C)	23	23	23	444	538
a (Å)	8.797(5)	8.789(6)	8.717(6)	8.852(4)	8.860(4)
b (Å)	5.852(2)	5.843(3)	5.805(3)	5.882(3)	5.888(3)
c (Å)	13.126(6)	13.127(8)	13.036(9)	13.194(6)	13.201(7)
V (Å³)	675.7(9)	674.1(11)	659.6(12)	687.0(9)	688.7(10)
No. refl.	2022	1115	654	754	723
No. unique ($I > 3\sigma_I$)	689	359	176	380	370
No. par.	52	21	21	52	46
R_{eq}	1.9	5.0	7.5	6.0	9.4
Scan speed (°/s)	0.04–0.08	0.04	0.04	0.04–0.08	0.04–0.08
R (F)* (%)	2.4	4.9	5.6	5.8	6.0
GoF**	1.20	1.12	1.28	1.20	1.23

Note: Variable scan speed was employed to improve counting statistics.
* $R(F) = \Sigma||F_o| - |F_c||/\Sigma|F_o|$.
** $GoF = [\Sigma w_i (F_o^2 - F_c^2)^2/(N - P)]^{1/2}$.

EXPERIMENTAL TECHNIQUES

The specimen used in this study was from the lawsonite type locality, Tiburon Peninsula, Marin County, California (USNM R3922). The same sample was used by Baur (1978) for his structural refinement. Chemical analysis, with the use of a scanning electron microscope equipped with an energy-dispersive X-ray spectrometer, agrees with the microprobe analysis of Baur (1978) and shows that the sample is homogeneous and very close to ideal composition.

Diffraction data were collected at room conditions from a crystal with dimensions 0.15 × 0.18 × 0.06 mm with the use of a four-circle Philips PW1100 diffractometer and graphite monochromatized Mo$K\alpha$ radiation (λ = 0.7107 Å). A total of 2022 integrated intensities from two equivalent sets with indices *hkl* and $\bar{h}kl$ (up to 40° θ) were collected for structural refinement (Table 1). After the merging of equivalent reflections (R_{eq} = 1.9%), 689 independent reflections were obtained with intensities higher than 3σ. Anisotropic refinement in space group *Ccmm* was performed using the SHELXL93 program (Sheldrick 1993). At that stage of refinement, two peaks in Fourier-difference maps were assigned to the H atom of the OH group (O4-H) and to the H atom of the H_2O molecule (HW-O5-HW). Further refinement cycles, including H-atom contribution, improved the agreement index and resulted in a final unweighted *R* of 2.4% for 52 parameters. Final atomic coordinates and displacement parameters are listed in Table 2; observed and calculated structure factors are listed in Table 3.[1]

High-*P* experimental study

A Merrill-Bassett diamond-anvil cell (DAC) with ⅛ carat diamonds was used for the high-pressure study. An Sm^{2+}:BaFCl powder for pressure calibration (Comodi and Zanazzi 1993a) and a 4:1 methanol : ethanol mixture used as a pressure-transmitting medium were introduced into the DAC together with the sample of lawsonite. Pressure was monitored by measuring the wavelength shift of the Sm^{2+} line excited by a 100 mw argon laser and detected by a 100 cm Jarrell-Ash optical spectrometer. The precision of the pressure measurements was 0.5 kbar. Steel foil 250 μm thick, with a hole of 300 μm diameter, was used as gasket material. The lattice parameters of two crystals from the same sample were determined at various pressures between 0.001 and 37.7 kbar (Table 4) by applying the least-squares method to the Bragg angles of about 30 reflections.[1] To avoid errors resulting from mechanical offset of the diffractometer and the sample, the centroid of each reflection was located by scanning on the positive and negative parts of the ω circle, and the results were averaged. Attempts to reach higher pressure failed because of destruction of the sample material.

Intensity data from the orthorhombic *C*-centered cell were collected at 28.7 kbar up to 35° θ, adopting nonbisecting geometry (Denner et al. 1978) and a 2.5° ω scan mode; data were corrected for pressure-cell absorption by an experimental attenuation curve (Finger and King 1978). Because systematic errors may be introduced by comparison of refinement results obtained from reflections for the whole reciprocal lattice measured at room conditions with results obtained from reflections from a limited part of reciprocal space (Glinnemann 1990) measured with the DAC, the same set of intensity data was collected at 0.5 kbar from the same crystal (0.12 × 0.12 × 0.05 mm) with the use of the same procedure.

Intensity data were analyzed with a digital procedure (Comodi et al. 1994), visually inspected to eliminate errors resulting from the overlap of diffraction effects from various parts of the diamond cell or by shadowing from the gasket, and merged into an independent data set.

The structure was refined in space group *Ccmm* with individual isotropic atomic displacement parameters using the SHELXL93 program. Details of the refinements are listed in Table 1; final fractional atomic positions and

[1] A copy of Tables 3 and 4 may be ordered as Document AM-96-616 from the Business Office, Mineralogical Society of America, 1015 Eighteenth Street NW, Suite 601, Washington, DC 20036, U.S.A. Please remit $5.00 in advance for the microfiche.

TABLE 2. Atomic fractional coordinates and anisotropic displacement factors (Å²)

Atom	*x*	*y*	*z*	U_{11}/U_{iso}	U_{22}	U_{33}	U_{23}	U_{13}	U_{12}
Ca	0.3331(1)	0	¼	0.0124(2)	0.0098(2)	0.0084(2)	0	0	0
	0.3330(1)	0	¼	0.0102(4)	—	—	—	—	—
	0.3322(4)	0	¼	0.0122(9)	—	—	—	—	—
	0.3327(2)	0	¼	0.026(1)	0.019(1)	0.018(1)	0	0	0
	0.3326(3)	0	¼	0.031(1)	0.025(1)	0.036(1)	0	0	0
Al	¼	¼	0	0.0060(2)	0.0059(2)	0.0058(2)	0.0002(2)	−0.0003(2)	−0.0004(1)
	¼	¼	0	0.0058(4)	—	—	—	—	—
	¼	¼	0	0.0073(8)	—	—	—	—	—
	¼	¼	0	0.0116(9)	0.008(1)	0.010(1)	0.0004(7)	−0.0019(6)	−0.0011(9)
	¼	¼	0	0.014(1)	0.010(1)	0.027(1)	0.0000(9)	−0.0024(7)	−0.0019(8)
Si	0.9805(1)	0	0.1330(1)	0.0053(2)	0.0062(2)	0.0051(2)	0	0.0000(1)	0
	0.9802(2)	0	0.1329(1)	0.0057(4)	—	—	—	—	—
	0.9797(3)	0	0.1334(2)	0.0084(8)	—	—	—	—	—
	0.9798(2)	0	0.1330(1)	0.0099(9)	0.0087(9)	0.0084(8)	0	0.0003(6)	0
	0.9799(2)	0	0.1329(2)	0.0111(9)	0.0110(9)	0.024(1)	0	0.0000(7)	0
O1	0.0496(2)	0	¼	0.0086(6)	0.0146(7)	0.0051(6)	0	0	0
	0.0499(6)	0	¼	0.0075(9)	—	—	—	—	—
	0.051(1)	0	¼	0.0054(2)	—	—	—	—	—
	0.0467(8)	0	¼	0.022(3)	0.027(4)	0.004(3)	0	0	0
	0.046(1)	0	¼	0.031(4)	0.031(5)	0.017(4)	0	0	0
O2	0.3788(1)	0.2727(1)	0.1170(1)	0.0095(3)	0.0085(3)	0.0086(3)	0.0014(3)	−0.0019(3)	−0.0021(3)
	0.3797(3)	0.2722(5)	0.1173(2)	0.0090(6)	—	—	—	—	—
	0.3776(6)	0.273(3)	0.1179(4)	0.011(1)	—	—	—	—	—
	0.3796(4)	0.2728(6)	0.1167(2)	0.016(2)	0.010(2)	0.017(2)	0.001(1)	−0.005(1)	−0.004(1)
	0.3793(4)	0.2736(7)	0.1168(3)	0.020(2)	0.015(2)	0.032(2)	0.000(2)	−0.005(2)	−0.004(2)
O3	0.1375(1)	0	0.0651(1)	0.0072(4)	0.0082(4)	0.0066(5)	0	0.0011(4)	0
	0.1378(4)	0	0.0646(2)	0.0072(7)	—	—	—	—	—
	0.1370(9)	0	0.0644(6)	0.012(2)	—	—	—	—	—
	0.1374(5)	0	0.0659(3)	0.012(2)	0.015(3)	0.011(2)	0	0.000(2)	0
	0.1373(6)	0	0.0658(4)	0.014(2)	0.019(3)	0.028(3)	0	0.000(2)	0
O4	0.6394(1)	0	0.0478(1)	0.0079(4)	0.0090(5)	0.0120(5)	0	0.0025(4)	0
	0.6385(4)	0	0.0481(2)	0.0103(7)	—	—	—	—	—
	0.6358(9)	0	0.0475(6)	0.0120(2)	—	—	—	—	—
	0.6406(6)	0	0.0474(4)	0.008(2)	0.010(2)	0.019(2)	0	0.0031(19)	0
	0.6396(6)	0	0.0466(4)	0.014(2)	0.013(3)	0.034(3)	0	0.0074(22)	0
O5	0.6092(2)	0	¼	0.0145(9)	0.039(1)	0.0112(8)	0	0	0
	0.6094(7)	0	¼	0.017(1)	—	—	—	—	—
	0.610(1)	0	¼	0.019(3)	—	—	—	—	—
	0.611(1)	0	¼	0.039(5)	0.066(7)	0.020(4)	0	0	0
	0.613(1)	0	¼	0.046(6)	0.079(9)	0.035(6)	0	0	0
HW	0.668(5)	0	0.301(4)	0.09(2)	—	—	—	—	—
H	0.556(7)	0	0.058(5)	0.11(2)	—	—	—	—	—

Note: For each atom, values from top to bottom correspond to room conditions, 0.5 kbar, 28.7 kbar, 444 °C, and 538 °C refinements, respectively. Estimated standard deviations are in parentheses and refer to the last digit. Isotropic temperature factors are reported for high-pressure refinements and H atoms.

displacement parameters are presented in Table 2. Observed and calculated structure factors are listed in Table 3.

High-*T* experimental study

For the high-temperature study, we used a microfurnace constructed in our laboratory and described in Comodi and Zanazzi (1993b). The temperature of the heating device was calibrated by the thermal expansion of an NaCl crystal (Pathak and Vasavada 1970). The crystals were attached to silica fibers with ceramic cement (M-Bond GA-100 cement, M-M Division, Measurements Group Inc., Raleigh, North Carolina). To monitor the sample temperature, a single NaCl crystal was mounted on the silica fiber together with the lawsonite crystal, and its *a* lattice parameter was determined at each temperature from the angular θ value of ~30 reflections. The precision of temperature measurements was better than ±5 °C. Two hours were allowed for equilibration at each temperature. The lattice parameters of four lawsonite fragments, with dimensions in the range 0.10–0.20 mm, were measured in air at several temperatures between 23 and 598 °C (Table 4). Above 540 °C, the reflection intensities dropped drastically to one-tenth of their initial values, and the sample turned reddish in color. This effect was irreversible when temperature was decreased.

Intensity data sets for the structural study were measured at ambient *P*, at 444 and 538 °C, from the same fragment and with the heating device assembled in the same way. Anisotropic atomic displacement parameters were used for all atoms except H. During data collection at 538 °C, the intensity of three reference reflections, monitored every 100 min, decreased by ~30% of their initial value. Data were therefore corrected for intensity decay on the basis of linear variations in the intensity of the reference reflections. Because reflection intensities are not affected in the same way by thermal damage, this may introduce a bias in the quality of the data.

Details on data collections and refinements are shown in Table 1, atomic coordinates in Table 2, and observed and calculated structure factors in Table 3.

TABLE 5. Bond distances (Å) and volumes (Å³) of coordination polyhedra of lawsonite at various pressures and temperatures

P (kbar)	0.001	0.5	28.7	0.001	0.001
T (°C)	23	23	23	444	538
Ca-O2 × 4	2.400(1)	2.394(3)	2.373(11)	2.417(3)	2.420(4)
Ca-O5	2.429(2)	2.429(7)	2.421(13)	2.465(10)	2.483(12)
Ca-O1	2.494(2)	2.488(5)	2.453(10)	2.532(8)	2.540(8)
Ca-O3 × 2	2.975(1)	2.978(3)	2.958(8)	2.981(5)	2.985(6)
$\langle Ca\text{-}O\rangle_{Avg.\ of\ 6}$	2.421	2.416	2.394	2.444	2.451
$\langle Ca\text{-}O\rangle_{Avg.\ of\ 8}$	2.559	2.556	2.535	2.578	2.584
V_{CaO_8}	24.33(5)	24.2(2)	23.6(3)	24.9(1)	25.2(2)
Al-O4 × 2	1.866(1)	1.869(2)	1.866(5)	1.869(3)	1.872(3)
Al-O2 × 2	1.913(1)	1.921(2)	1.901(5)	1.925(3)	1.927(4)
Al-O3 × 2	1.962(1)	1.956(2)	1.945(5)	1.978(3)	1.979(4)
⟨Al-O⟩	1.914	1.915	1.904	1.924	1.926
V_{AlO_6}	9.19(1)	9.22(3)	9.07(7)	9.33(4)	9.36(5)
Si-O2 × 2	1.616(1)	1.611(3)	1.604(14)	1.619(2)	1.617(3)
Si-O3	1.644(1)	1.650(4)	1.640(9)	1.652(3)	1.652(6)
Si-O1	1.652(1)	1.655(2)	1.641(5)	1.653(3)	1.653(4)
⟨Si-O⟩	1.632	1.632	1.622	1.636	1.635
V_{SiO_4}	2.225(4)	2.21(1)	2.18(4)	2.23(1)	2.23(2)
H-O4	0.75(4)				
HW-O5	0.84(4)				
O4-O2	2.937(9)	2.92(2)	2.90(2)	2.96(2)	2.96(2)
O5-O4	2.667(9)	2.66(2)	2.65(2)	2.69(2)	2.70(2)

Note: The polyhedral volumes were computed using the program VOLCAL (Hazen and Finger 1982).

RESULTS AT ROOM CONDITIONS

The results of our anisotropic structural refinement at room conditions are in good agreement with those of Baur (1978). Relevant bond lengths are listed in Table 5. However, we succeeded in locating both H atoms. They are very close to the H positions derived from geometric and electrostatic considerations (Baur 1978). In fact, the theoretical position of the H atom of the OH group differed by only 0.17 Å from the position determined by our X-ray refinement. Similarly, the calculated H-atom position of the H_2O molecule differed from the position determined by X-ray diffraction by only 0.16 Å.

The OH groups (O4-H) and the H_2O molecule (HW-O5-HW) were located in the (010) symmetry plane, the OH groups being perpendicular to the chains of Al octahedra, which is in agreement with the IR spectroscopic data of Labotka and Rossman (1974) and Le Cleac'H and Gillet (1990). The OH group forms a hydrogen bond with O4′ oxygen atom, the O4-O4′ distance being 2.775 Å. Another bifurcated, weaker hydrogen bond probably forms between OH and both O2 and O2′ (both O4-O2 and O4-O2′ are 2.937 Å). The O5-O4 distance of 2.667 Å is also indicative of a hydrogen bond between the O atom of the H_2O molecule and that of the OH group.

TABLE 6. Bond-valence calculations for lawsonite at room conditions, according to Brown and Altermatt (1985)

	Ca	Al	Si	H	Hw	Σ
O1	0.241		0.927 × 2			2.09
O2	0.310	0.493	1.022	0.12		1.95
O3	0.066	0.432 × 2	0.947			1.88
O4		0.559 × 2		0.76	0.21	2.09
O5	0.287				0.79 × 2	1.87

This hydrogen-bond scheme produces fairly good electrostatic balance of all O atoms and cations, as is evident from a bond-valence calculation (Brown and Altermatt 1985) reported in Table 6.

HIGH-P RESULTS

Lawsonite deforms linearly (Fig. 1) and with an almost isotropic compression of the cell edges in the pressure range analyzed. The compressibility coefficients of the lattice parameters are $\beta_a = 3.4(1) \times 10^{-4}$, $\beta_b = 3.0(1) \times 10^{-4}$, $\beta_c = 2.8(2) \times 10^{-4}$ kbar^{-1}. The bulk modulus, calculated as the reciprocal of cell-volume compressibility, is 1100(40) kbar. If the isothermal bulk modulus is calculated by means of the BIRCH 2.0 program (Ross and Webb 1990), from the fit of pressure vs. volume data to a Birch-Murnaghan equation of state by a nonlinear least-squares method, and $K' = 4$, the value is 960(20) kbar.

Our results agree with the bulk modulus calculated by Holland and Powell (1990) on the basis of Wang's method (Wang 1978). Holland and Powell found the equation of state to be $V/V_0 = 1 - 8.9 \times 10^{-7}P$ (bar), where, considering $V_0 = 10.132$ J/bar, the calculated bulk modulus is 1100 kbar. The bulk modulus of lawsonite—which is significantly higher than that of anorthite (833 kbar; Hackwell and Angel 1992), although the two minerals have similar chemical content—confirms the importance of cation and anion coordination on high-pressure behavior, as observed in several other phases. Moreover, the results show that the bulk modulus is proportional to packing efficiency, expressed as the volume occupied by each O atom (Ungaretti 1991). This value is 20.9 Å³ for anorthite and 16.9 Å³ for lawsonite. The bulk modulus of lawsonite is intermediate between the values of other high-P–low-T minerals, such as ellenbergerite ($K = 1330$

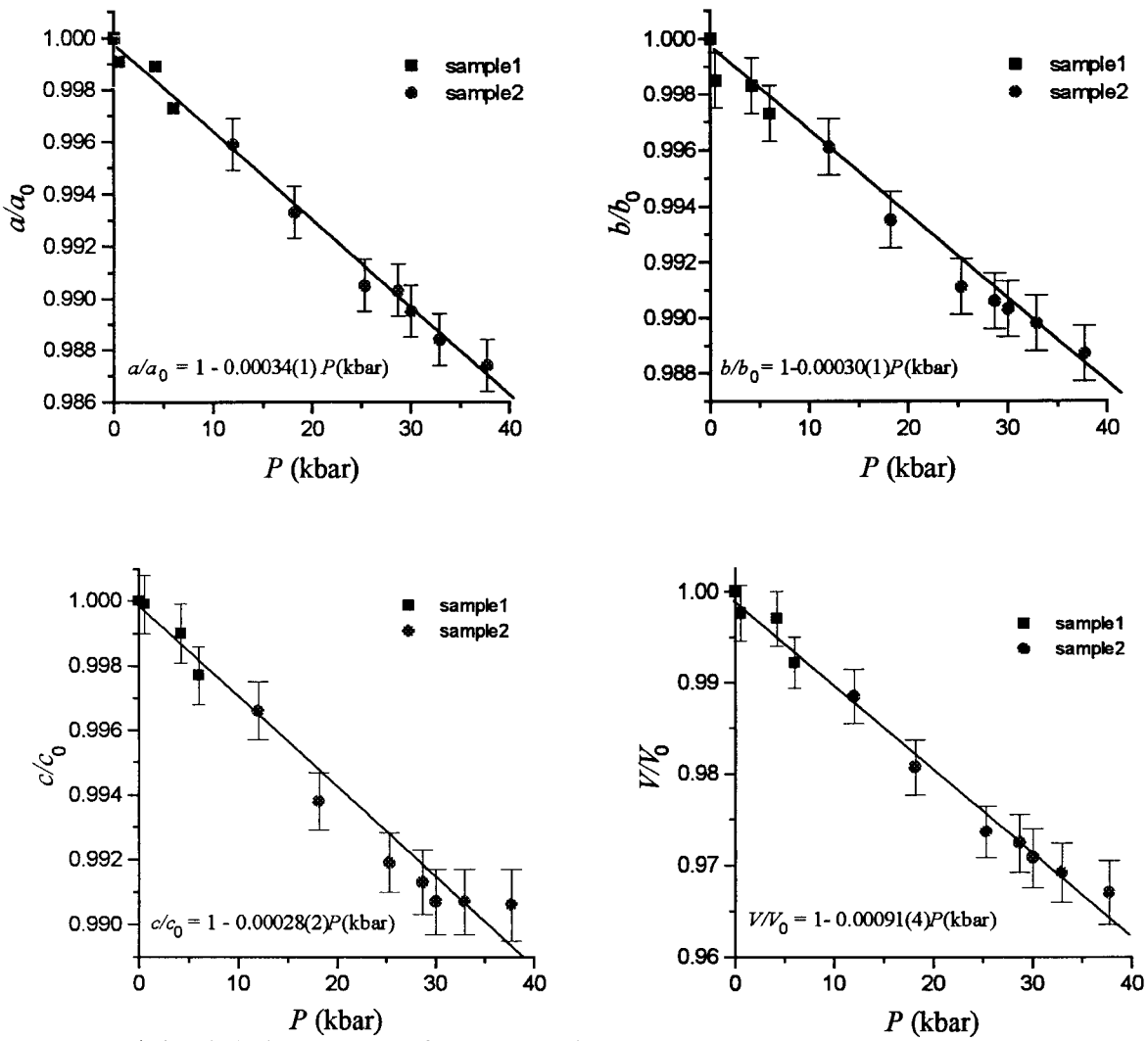

FIGURE 1. Variations in lattice parameters of two samples of lawsonite at various pressures normalized to the room-pressure value. Estimated error of P is 0.5 kbar.

kbar, Comodi and Zanazzi 1993c), magnesiochloritoid (K = 1480 kbar, Comodi et al. 1992), and glaucophane (K = 960 kbar, Comodi et al. 1991).

Comparison of structural refinements at 0.5 and 28.7 kbar (Table 5) shows that the Si tetrahedra are almost incompressible in this P range at room temperature, whereas the Al octahedra have a bulk modulus of 1720 kbar. The latter become more regular with increasing P: The common O3-O4 edge, which is very short at room conditions [2.46(2) Å], does not change with increasing P, whereas the mean unshared edges are reduced from 2.75(2) to 2.73(2) Å.

The distorted CaO_6 octahedra have a bulk modulus of 1140 kbar. This value compares well with those measured in phases containing Ca polyhedra. For example, Ross and Reeder (1992) measured K_{CaO_6} of 910 and 890 kbar in dolomite and ankerite, respectively, and Hazen and Finger (1978) measured a polyhedral bulk modulus of 1150 kbar for the eightfold coordinated Ca in grossular. In clinozoisite the ninefold and tenfold coordinated Ca have bulk moduli of 1170 and 870 kbar, respectively (Comodi and Zanazzi 1996).

An important aspect of lawsonite is the geometric evolution with P of the large cavities in which H_2O molecules are located. This may be evaluated by the amount of polyhedral tilting caused by the pressure increase, more than by variations of cation-O bond distances and bond angles. The (010) section of the channel is approximately ditrigonal at room conditions (see Fig. 2 in Libowitzky and Armbruster 1995), the mean difference between obtuse and acute angles, $\Delta\alpha$, being 63.0° (Table 7). From 0.5 to 28.7 kbar, tetrahedral rotation slightly increases ditrigonalization, and $\Delta\alpha$ becomes 64.6°. However, the compressibility of the cavity, estimated through the reduction of O2-O2′, O3-O3′, and O1-O1′ nonbonding distances (Table 7), is equal to that of the Ca polyhedra.

TABLE 7. Cavity evolution with P and T described through the variations in some O-O distances (Å) and angles (°)

P (kbar)	0.001	0.5	28.7	0.001	0.001
T (°C)	23	23	23	444	538
O2-O2′	3.492(4)	3.483(6)	3.445(8)	3.518(7)	3.517(7)
O3-O3′	4.855(4)	4.868(6)	4.84(1)	4.858(7)	4.863(8)
O1-O1′	5.283(9)	5.28(2)	5.24(2)	5.31(2)	5.32(2)
O2-O1-O2′	82.1(1)	82.0(2)	81.3(3)	82.8(2)	83.0(2)
O1-O2-O3	153.1(1)	153.3(2)	153.9(3)	152.2(2)	152.2(2)
O2-O3-O1	89.9(1)	89.7(2)	89.1(3)	90.8(2)	90.8(2)
O3-O1-O3′	144.7(1)	144.8(2)	145.5(3)	143.4(2)	143.1(2)
$\Delta\alpha$	63.0	63.3	64.6	61.0	60.7
Si-O1-Si′	136.8(1)	136.5(3)	135.6(6)	138.0(5)	138.6(6)

Note: The $\Delta\alpha$ is the difference between averages of obtuse and acute angles of channel (010) section. Prime symbol indicates atom position at $x,y,0.5-z$.

When pressure increases, the channels running parallel to the b axis are narrowed along the [001] direction by the decrease of the Si-O-Si′ angle, which changes from 136.8° at room pressure to 135.6 at 28.7 kbar (Table 7). This behavior is in agreement with that observed in other disilicates, e.g., clinozoisite (Comodi and Zanazzi 1996), in which the angle between the tetrahedral pairs decreases with increasing pressure. Because the high-P behavior of minerals is generally the opposite of their high-T behavior, the same structural evolution should be observed with high P or low T. A recent study of lawsonite at low temperature (Libowitzky and Armbruster 1995) shows good agreement with our data. In fact, a change in temperature from 295 to 110 K yields a change in the Si-O-Si′ angle from 136.8 to 135.8°.

Because of the low quality of the high-P structural refinements, direct location of H atoms was not achieved. However, indirect indications were obtained from the variations in distances between the O atoms involved in hydrogen bonding. Table 5 lists the O4-O2 and O4-O5 distances at various pressures. Their small variations indicate that OH groups and H_2O molecules do not change their configurations over about 28 kbar. The permanence of H_2O molecules in structural channels with P is estimated by analyzing the evolution of the cavity in which H_2O is hosted. A computer program (Mugnoli 1992) designed to search for empty spherical voids within a crystal structure was used. Ionic radii according to Shannon (1976) were introduced, together with the coordinates of all atoms with the exception of the O5 oxygen atom (from the H_2O molecule), as determined from refinements at room temperature and 0.5–28.7 kbar. The only cavity with a suitable diameter found by the program had its center on the O5 oxygen atom. Its radius changed from 1.26(2) Å at room conditions to 1.24(2) Å at 28.7 kbar. Therefore, the volume of the cavity in which the H_2O molecule is located changes by only about 5% over the P range investigated.

HIGH-T RESULTS

Thermal expansion was determined by a least-squares regression analysis of the lattice parameters of four crystal fragments, normalized to their respective values at 23 °C, vs. temperature (Fig. 2). The following equations were obtained: $a/a_0 = 1 + 1.26(4) \times 10^{-5}T$ (°C), $r^2 = 0.97$; $b/b_0 = 1 + 1.12(4) \times 10^{-5}T$ (°C), $r^2 = 0.96$; $c/c_0 = 1 + 7.6(3) \times 10^{-6}T$ (°C), $r^2 = 0.96$; and $V/V_0 = 1 + 3.13(9) \times 10^{-5}T$ (°C), $r^2 = 0.97$.

The mean thermal expansion coefficients, calculated between 20 and 600 °C, were $\alpha_a = 1.26(4) \times 10^{-5}$, $\alpha_b = 1.12(4) \times 10^{-5}$, $\alpha_c = 7.6(3) \times 10^{-6}$ °C^{-1}, with limited anisotropic behavior expressed as $\alpha_a:\alpha_b:\alpha_c = 1.66:1.47:1$. Our results are of the same order of magnitude as the values of $\alpha_a = 1.49 \times 10^{-5}$, $\alpha_b = 1.18 \times 10^{-5}$, $\alpha_c = 1.12 \times 10^{-5}$ °C^{-1} found from thermal dilatation measurements between 15 and 449 °C using powder diffraction techniques (Le Cleac'H 1990).

The drastic and irreversible reduction of reflection intensities observed above 500 °C was ascribed to damage caused by dehydration and indicated the breakdown of lawsonite under room pressure. This result was in agreement with the dynamic thermal behavior of lawsonite: The TGA curve showed two endothermic peaks at 630 and 760 °C (Coombs 1953), as a result of H_2O and OH loss. Moreover, recent TGA experiments (Libowitzky and Armbruster 1995) have shown that lawsonite starts to dehydrate at ~800 K.

The Si tetrahedra did not expand with T, changes being within 1σ (Table 5). The Al octahedra had a mean thermal expansion coefficient, α_V, of 3.6×10^{-5} °C^{-1}, which compares well with the expansion of Al octahedra in other phases with Al-octahedral chains such as Al_2SiO_5 polymorphs [e.g., Winter and Ghose (1979) measured an α_V of 3.6×10^{-5} °C^{-1} for Al octahedra in andalusite, and for the four Al octahedra in kyanite the range in values is $2.7–3.3 \times 10^{-5}$ °C^{-1}]. The Al octahedra did not change their distortion with T: The difference between unshared and shared edges was the same as that measured at room conditions. The thermal expansion coefficient of the Ca polyhedra, 6.5×10^{-5} °C^{-1}, was about double that of the Al polyhedra.

Polyhedral tilting with T decreased the "ditrigonalization" of the (010) section of the large channel: The mean difference between obtuse and acute angles, $\Delta\alpha$, became 60.7° at 538 °C (Table 7).

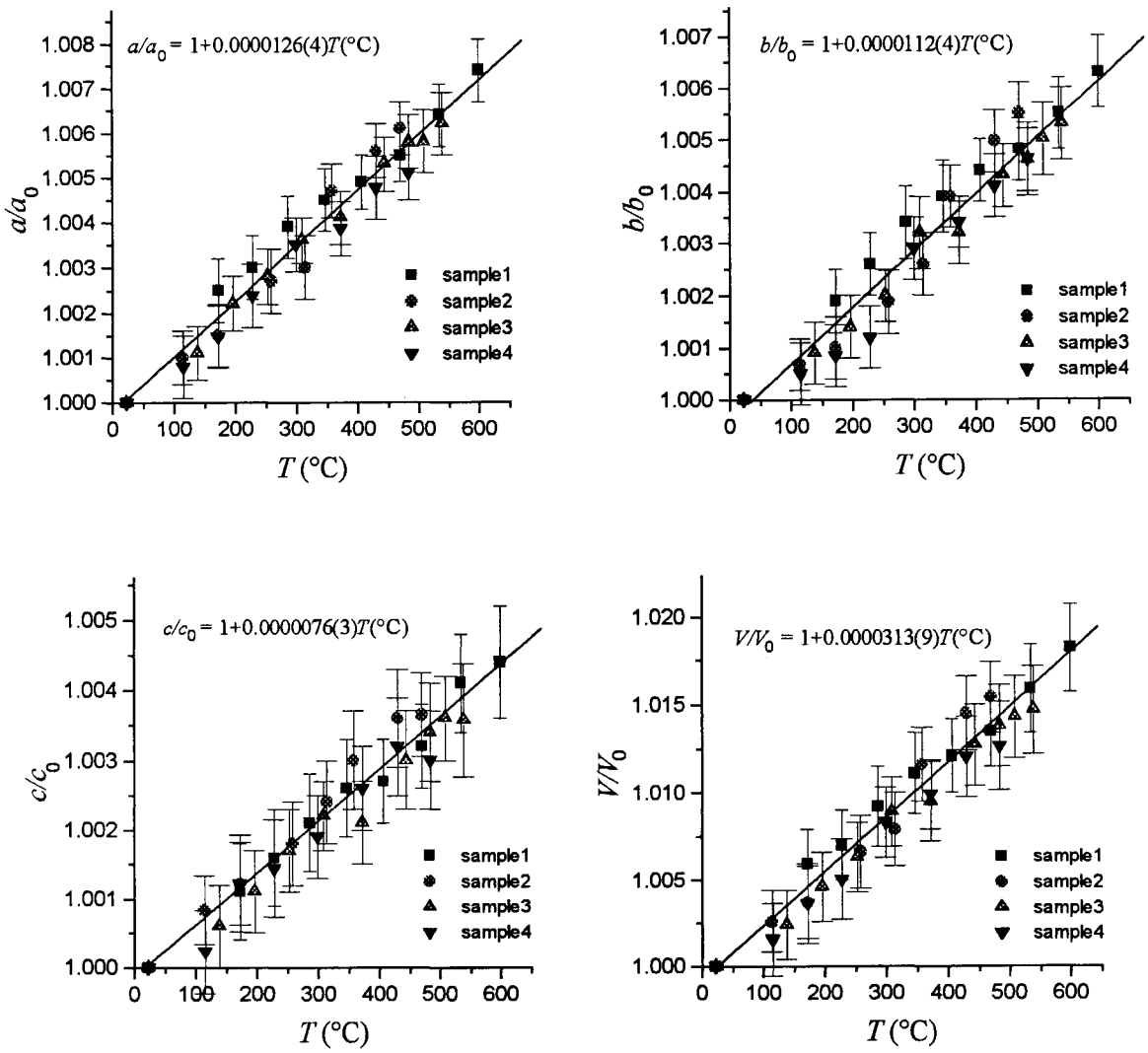

FIGURE 2. Variations in lattice parameters of four fragments of lawsonite at various temperatures normalized to the room-temperature value. Estimated error of T is 5 °C.

When the temperature changed from 23 to 538 °C, the Si-O1-Si′ angle increased from 136.8 to 138.6° (Table 7). Substituting a large cation in the channel had the same effect. In fact, the Si-O1-Si′ angle is 146.6° in the structure of hennomartinite, $SrMn_2[Si_2O_7](OH)_2 \cdot H_2O$, a new mineral of the lawsonite type (Armbruster et al. 1992, 1993), in which Ca is replaced by Sr, and Al is substituted by Mn^{3+}. This phenomenon has also been observed in other minerals with continuous channels, such as davyne, in which the substitution of K for Na produces structural deformations analogous to those observed with increasing temperature (Bonaccorsi et al. 1995).

Calculations of the evolution of the H_2O cavity, with the use of the same computer program used for the high-*P* data, showed that the empty spherical void, centered on the O5 oxygen atom, changed its radius from 1.26 Å at room conditions to 1.29 Å at 534 °C.

DISCUSSION AND CONCLUSIONS

Lawsonite represents a further example of the effects of structurally analogous intensive variables, namely, the type of structural changes that occur with changes in pressure are similar and opposite to those observed with changes in temperature. Moreover, the changes induced by the substitution of large ions in the channels are comparable to those induced by heating. The largest variations affect CaO_6 polyhedra, and to a minor extent AlO_6 octahedra; the channels running along *b* are narrowed by *P* and widened by *T*, and the Si-O1-Si′ angle is reduced and stretched.

The thermal behavior of lawsonite gives indications of the permanence of H_2O molecules in the structure at atmospheric pressure up to above 500 °C. Reflection intensities decrease only above that temperature, and struc-

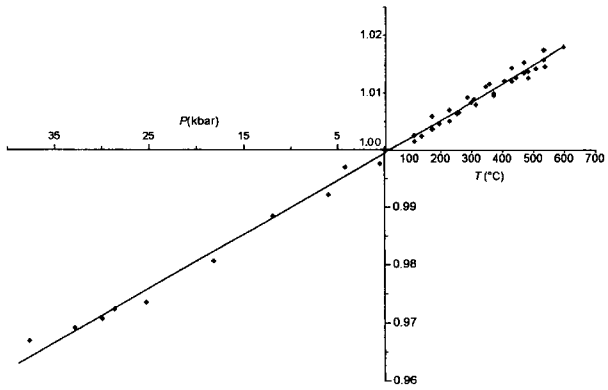

FIGURE 3. Cell volumes at various pressures and temperatures normalized to the room-condition value. P and T scales were arranged to obtain a linear fitting of high-P, high-T data.

tural refinement at 444 °C shows the same configuration of H atoms observed at 23 °C. So the breakdown of lawsonite at room pressure occurs above 500 °C. Moreover, the framework of octahedral-tetrahedral ribbons does not collapse in the H_2O cavity with pressure, but the diameter of the empty spherical void in which H_2O molecules are hosted decreases by only about 5% with a pressure increase of 28 kbar. The observed antisymmetric behavior of lawsonite with T and P shows that, at first approximation, the effects of pressure and temperature are cumulative, so that the following equation of state may be defined: $V/V_0 = 1 + 3.13(9) \times 10^{-5}T - 9.1(3) \times 10^{-4}P$, where T is in degrees Celsius and P is in kilobars.

To understand the structural evolution of the phase with depth, it is useful to calculate the α/β ratio. For lawsonite this value is 34 bar/°C, definitely higher than the mean geothermal gradient of 20 bar/°C. This P/T gradient, indicating the geometric invariance of the structure, is plotted in Figure 3, which shows cell-volume variations with T and P normalized to the room-condition value. In Figure 3 the scale is arranged to produce the best linear fit of both high-T and high-P data. The same volume variations, at absolute values, are obtained with increments, for example, of 500 °C and about 17 kbar. So, with an average geothermal gradient, lawsonite should expand with depth in the crust and become unstable. However, in high-pressure, low-temperature environments, i.e., ones with a gradient of about 10 °C/km, as in subducted oceanic crust (Davies and Stevenson 1992), the cell volume of lawsonite does not change with respect to that observed in room conditions. This result is in agreement with the values obtained for other minerals from high-P, low-T environments: For example, in ellenbergerite the α/β ratio is 33 bar/°C (Comodi and Zanazzi 1993c), and in magnesiochloritoid it is 43 bar/°C (Comodi et al. 1992).

The structural invariance conditions determined here indicate that although lawsonite may be stable even at great depths in P/T regimes characteristic of subduction slabs, it may become unstable during exhumation processes. For these reasons, lawsonite is rarely preserved and is generally found as a relict or pseudomorphosed in clinozoisite.

ACKNOWLEDGMENTS

We thank S. Poli who stimulated our interest in lawsonite. This research was made possible by the kind loan of the lawsonite sample by the Smithsonian Institution. We also thank V. Trommsdorff for his valuable comments and criticism, and T. Armbruster for sending us his results on low-temperature phase transitions of lawsonite before publication. The manuscript benefited from critical reviews by D.R. Allan and E. Libowitzky. This work was financially supported by CNR and MURST (40% and 60%, respectively).

REFERENCES CITED

Armbruster, T., Oberhänsli, R., and Bermanec, V. (1992) Crystal structure of $SrMn_2[Si_2O_7](OH)_2 \cdot H_2O$, a new mineral of the lawsonite type. European Journal of Mineralogy, 4, 17–22.

Armbruster, T., Oberhänsli, R., Bermanec, V., and Dixon, R. (1993) Hennomartinite and kornite, two new Mn^{3+} rich silicates from the Wessel Mine, Kalahari, South Africa. Schweizerische Mineralogische und Petrographische Mitteilungen, 73, 349–355.

Baur, W.H. (1978) Crystal structure refinement of lawsonite. American Mineralogist, 63, 311–315.

Bonaccorsi, E., Comodi, P., and Merlino, S. (1995) Thermal behaviour of davyne-group minerals. Physics and Chemistry of Minerals, 22, 367–374.

Brown, I.D., and Altermatt, D. (1985) Bond-valence parameters obtained from a systematic analysis of the inorganic crystal structure database. Acta Crystallographica, B41, 244–247.

Comodi, P., Mellini, M., Ungaretti, L., and Zanazzi, P.F. (1991) Compressibility and high pressure structure refinement of tremolite, pargasite and glaucophane. European Journal of Mineralogy, 3, 485–499.

Comodi, P., Mellini, M., and Zanazzi, P.F. (1992) Magnesiochloritoid: Compressibility and high pressure structure refinement. Physics and Chemistry of Minerals, 18, 483–490.

Comodi, P., and Zanazzi, P.F. (1993a) Improved calibration curve for the Sm^{2+}:BaFCl pressure sensor. Journal of Applied Crystallography, 26, 843–845.

——— (1993b) Structural study of ellenbergerite: Part I. Effect of high temperature. European Journal of Mineralogy, 5, 819–829.

——— (1993c) Structural study of ellenbergerite: Part II. Effect of high pressure. European Journal of Mineralogy, 5, 831–838.

Comodi, P., Melacci, P.T., Polidori, G., and Zanazzi, P.F. (1994) Trattamento del profilo di diffrazione da campioni in cella ad alta pressione. Proceedings of XXIV National Congress of Associazione Italiana di Cristallografia, Pavia, September 27–29, 119–120.

Comodi, P., and Zanazzi, P.F. (1996) High pressure structural behaviour of some minerals of the epidote group. EMPG-VI Meeting, April 10–13, Bayreuth.

Coombs, D.S. (1953) The pumpellyite mineral series. Mineralogical Magazine, 30, 113–135.

Davies, J.H., and Stevenson, D.J. (1992) Physical model of source region of subduction zone volcanics. Journal of Geophysical Research, 97, 2037–2070.

Denner, W., Schulz, H., and d'Amour, H. (1978) A new measuring procedure for data collection with a high-pressure cell on X-ray four-circle diffractometer. Journal of Applied Crystallography, 11, 260–264.

Diessel, C.F.K., Brothers, R., and Black, P.M. (1978) Coalification and graphitization in high-pressure schists in New Caledonia. Contributions to Mineralogy and Petrology, 68, 63–78.

Finger, L.W., and King, H. (1978) A revised method of operation of the single-crystal diamond cell and refinement of the structure of NaCl at 32 kbar. American Mineralogist, 63, 337–342.

Glinnemann, J. (1990) Future prospects of laboratory diamond-anvil-cell work. XVth Congress I.U.Cr., July 19–28, Bordeaux, France, Abstracts, C-354.

Hackwell, T.P., and Angel, R.J. (1992) The comparative compressibility

of reedmergnerite, danburite and their aluminium analogues. European Journal of Mineralogy, 4, 1221–1227.

Hazen, R.M., and Finger, L.W. (1978) Crystal structures and compressibilities of pyrope and grossular to 60 kbar. American Mineralogist, 63, 297–303.

——— (1982) Comparative crystal chemistry, 231 p. Wiley, New York.

Holland, T.J.B., and Powell, R. (1990) An enlarged and updated internally consistent thermodynamic dataset with uncertainties and correlations: The systems K_2O-Na_2O-CaO-MgO-MnO-FeO-Fe_2O_3-Al_2O_3-TiO_2-SiO_2-C-H_2-O_2. Journal of Metamorphic Geology, 8, 89–124.

Labotka, T.C., and Rossman, G.R. (1974) The infrared pleochroism of lawsonite: The orientation of the water and hydroxide groups. American Mineralogist, 59, 799–806.

Le Cleac'H, A. (1990) Contribution à l'étude des propriétés des minéraux à haute pression: Spectroscopie et calcul des grandeurs thermodynamiques de la lawsonite, des épidotes et des polymorphes de SiO_2. Mémoires et Documentes du Centre Armoricain d'Etude Structurale des Socles, Rennes, 32, 190 p.

Le Cleac'H, A., and Gillet, P. (1990) IR and Raman spectroscopic study of natural lawsonite. European Journal of Mineralogy, 2, 43–53.

Libowitzky, E., and Armbruster, T. (1995) Low-temperature phase transitions and the role of hydrogen bonds in lawsonite. American Mineralogist, 80, 1277–1285.

Mugnoli, A. (1992) A micro-computer program to survey empty spaces in a crystal structure. Abstracts of 14th European Crystallographic Meeting, August 2–7, Enschede, the Netherlands, 530.

Pathak, P.D., and Vasavada, N.G. (1970) Thermal expansion of NaCl, KCl and CsBr by X-ray diffraction and the law of corresponding states. Acta Crystallographica, A26, 655–658.

Pawley, A.R. (1994) The pressure and temperature stability limits of lawsonite: Implications for H_2O recycling in subduction zones. Contributions to Mineralogy and Petrology, 118, 99–108.

Poli, S., and Schmidt, M.W. (1995) H_2O transport and release in subduction zones: Experimental constraints on basaltic and andesitic systems. Journal of Geophysical Research, 100, 22299–22314.

Ross, C.R., II, and Webb, S.L. (1990) BIRCH, a program for fitting *PV* data to an Eulerian finite-strain equation of state. Journal of Applied Crystallography, 23, 439–440.

Ross, N.L., and Reeder, R.J. (1992) High-pressure structural study of dolomite and ankerite. American Mineralogist, 77, 412–421.

Schmidt, M.W. (1995) Lawsonite: Upper pressure stability and formation of higher density hydrous phases. American Mineralogist, 80, 1286–1292.

Schmidt, M.W., and Poli, S. (1994) The stability of lawsonite and zoisite at high pressure: Experiments in CASH to 92 kbar and implications for the presence of hydrous phases in subducted lithosphere. Earth and Planetary Science Letters, 124, 105–118.

Shannon, R.D. (1976) Revised effective ionic radii and systematic studies of interatomic distances in halides and chalcogenides. Acta Crystallographica, A32, 751–767.

Sheldrick, G.M. (1993) SHELXL93: Program for the refinement of crystal structures. University of Göttingen, Germany.

Ungaretti, L. (1991) Crystal-chemical information: Site geometry and site population. Proceedings of V Summer School on "Pressure and temperature evolution of orogenic belts," September, Siena, Italy, 235–247.

Wang, H.F. (1978) Elastic constant systematics. Physics and Chemistry of Minerals, 3, 251–261.

Wickman, F.E. (1947) The crystal structure of lawsonite $CaAl_2(Si_2O_7)(OH)_2 \cdot H_2O$. Arkiv för Kemie Mineralogi och Geologi, 25A(2), 1–7.

Winter, J.K., and Ghose, S. (1979) Thermal expansion and high-temperature crystal chemistry of the Al_2SiO_5 polymorphs. American Mineralogist, 64, 573–586.

MANUSCRIPT RECEIVED JULY 7, 1995
MANUSCRIPT ACCEPTED MARCH 19, 1996